Phase Behavior and Rheological Properties of Polyelectrolyte Inks for Direct-Write Assembly

Gregory M. Gratson† and Jennifer A. Lewis*,†,‡

Materials Science and Engineering Department, Chemical and Biomolecular Engineering Deparment, and Frederick Seitz Materials Research Laboratory, University of Illinois at Urbana-Champaign, Urbana, Illinois 61801

Received July 14, 2004. In Final Form: September 6, 2004

Three-dimensional (3-D) structures with micron-sized features have been fabricated via the direct-write assembly of polyelectrolyte inks[1]. By mixing oppositely charged species under solution conditions that promote polyelectrolyte exchange reactions, we have created concentrated fluids capable of flowing through microscale deposition nozzles. Ink deposition into an alcohol/water coagulation reservoir yielded polyelectrolyte filaments that rapidly solidify to enable three-dimensional patterning of microperiodic structures with self-supporting features. The influence of ink and reservoir chemistry on the phase behavior, rheological properties, and assembly of concentrated polyelectrolyte complexes is reported with an emphasis on the optimal conditions for 3-D writing.

Introduction

There is intense interest in fabricating three-dimensional (3-D) microperiodic structures comprised of polymeric,[1−3] colloidal,[4] or semiconductor[5] materials due to their potential application as microfluidic networks,[6] tissue engineering scaffolds,[7] drug-delivery devices,[8] sensors,[9] and photonic band gap materials.[10] These applications either require[9,10] or could benefit from[6−8] the ability to pattern micron-sized features in complex 3-D architectures. Several strategies have been introduced for precisely assembling materials into 3-D periodic arrays at the microscale,[1−5] including standard lithographic,[5] laser-based polymerization,[2,3] epitaxial assembly,[4] and, most recently, ink writing[1] techniques. Of these, only the latter approach offers the materials flexibility, low cost, and ability to construct arbitrary 3-D structures required for advances across multidisciplinary boundaries.

Direct-write techniques[11] that involve the layer-by-layer assembly of materials via "ink" deposition offer a flexible, inexpensive route for creating complex 3-D structures. We recently reported the direct-write assembly of 3-D microperiodic structures using concentrated polyelectrolyte inks.[1] Unlike our prior efforts,[6,12−14] these inks consist of viscous fluids that flow through microscale deposition nozzles (∼1 μm in diameter) and then rapidly coagulate in a deposition reservoir to form 3-D structures with self-supporting features. This ink design utilizes concentrated polyelectrolyte complexes[15] comprised of polyanion/polycation mixtures in an aqueous solution. These oppositely charged species typically phase separate to form an aggregated network with a stoichiometric ratio of anionic to cationic charge groups. However, soluble complexes can be formed from nonstoichiometric mixtures under specific conditions.[16]

Polyelectrolyte complexes exhibit a rich phase behavior that depends on several factors, including the polyelectrolyte type and architecture, their individual molecular weight and molecular weight ratio, the polymer concentration and mixing ratio, the ionic strength and pH of the solution, and the mixing conditions.[15] This vast array of experimental parameters makes it difficult to derive universal models for polyelectrolyte complex formation, but some trends have been reported.[17−20] Three types of phase behavior have been observed upon mixing oppositely charged polyelectrolytes together in solution: (1) a macroscopically homogeneous, soluble complex (single-phase), (2) a turbid suspension comprised of stable complex colloidal particles in a polymer-poor fluid (two-phase), or (3) a precipitated complex with a polymer-poor supernatant fluid (two-phase).[15] To create the desired ink fluidity, soluble complexes comprised of different molecular weight polyions must be mixed together at a nonstoichiometric

* Corresponding author. E-mail address: jalewis@uiuc.edu.
† Materials Science and Engineering Deparment and Frederick Seitz Materials Research Laboratory.
‡ Chemical and Biomolecular Engineering Department.

(1) Gratson, G. M.; Xu, M.; Lewis, J. A. *Nature* **2004**, *428*, 386.
(2) Campbell, M.; Sharp, D. N.; Harrison, M. T.; Denning, R. G.; Turberfield, A. J. *Nature* **2000**, *404*, 53−56.
(3) Cumpston, B. H.; Ananthavel, S. P.; Barlow, S.; Dyer, D. L.; Ehrlich, J. E.; Erskine, L. L.; Heikal, A. A.; Kuebler, S. M.; Lee, I.-Y. S.; McCord-Maughon, D.; Qin, J.; Marder, S. R.; Perry, J. W. *Nature* **1999**, *398*, 51−54.
(4) van Blaaderen, A.; Ruel, R.; Wiltzius, P. *Nature* **1997**, *385*, 321−324.
(5) Lin, S. Y.; Fleming, J. G.; Hetherington, D. L.; Smith, B. K.; Biswas, R.; Ho, K. M.; Sigalas, M. M.; Zubrzycki, W.; Kurtz, S. R.; Bur, J. *Nature* **1998**, *394*, 251−253.
(6) Therriault, D.; White, S. R.; Lewis, J. A. *Nat. Mater.* **2003**, *2*, 265−271.
(7) Griffith, L. G.; Naughton, G. *Science* **2002**, *295*, 1009−1014.
(8) Li, Y. Y.; Barlow, S.; Sailor, M. J.; Tan, K. H.; Zehner, R. W.; Marder, S. R. *Science* **2003**, *299*, 2045−2047.
(9) Asher, S. A.; Alexeev, V. L.; Goponenko, A. V.; Sharma, A. C.; Lednev, I. K.; Wilcox, C. S.; Finegold, D. N. *J. Am. Chem. Soc.* **2003**, *125*, 3322−3329.
(10) Joannopoulos, J. D.; Villeneuve, P. R.; Fan, S. *Nature* **1997**, *386*, 143−149.
(11) Chrisey, D. B. *Science* **2000**, *289*, 879−881.
(12) Smay, J. E.; Cesarano, J.; Lewis, J. A. *Langmuir* **2002**, *18*, 5429−5437.
(13) Smay, J. E.; Gratson, G. M.; Sheperd, R. F.; Cesarano, I. J.; Lewis, J. A. *Adv. Mater.* **2002**, *14*, 1279−1283.
(14) Li, Q.; Lewis, J. A. *Adv. Mater.* **2003**, *15*, 1639−1643.
(15) Philipp, B.; Dautzenberg, H.; Linow, K.-J.; Koetz, J.; Dawydoff, W. *Prog. Polym. Sci.* **1989**, *14*, 91−172.
(16) Zezin, A. B.; Kabanov, V. A. *Russ. Chem. Rev.* **1982**, *51*, 833−855.
(17) Michaels, A. S. *Ind. Eng. Chem.* **1965**, *57*, 32−40.
(18) Abe, K.; Ohno, H.; Tsuchida, E. *Makromol. Chem.* **1977**, *178*, 2285−2293.
(19) Zheleznova, I. V.; Shulbaeva, G. B.; Kalyuzhnaya, R. I.; Zezin, A. B.; Kabanov, V. A. *Dokl. Akad. Nauk SSSR* **1986**, *287*, 662−666.
(20) Karibyants, N.; Dautzenberg, H.; Colfen, H. *Macromolecules* **1997**, *30*, 7803−7809.

10.1021/la048228d CCC: $30.25
Published on Web 12/07/2004

ratio of ionizable groups, with the higher molecular weight (M_w) species in excess in solution. They must also be mixed together under ionic strength conditions that promote polyelectrolyte exchange reactions to yield a homogeneous fluid.[21]

Polyelectrolyte complexes play a central role in other layer-by-layer (LbL) assembly routes.[22] Both functional thin films and novel core−shell particles[23] have recently been assembled through the sequential adsorption of oppositely charged polyelectrolytes from dilute solution onto flat or spherical surfaces, respectively. These structures have been fabricated using biological[24] or optically[25] active polymers, into which other charged species, for example, nanoparticles[26] or dyes,[27] may be incorporated. By exploiting soft lithographic techniques, such as polymer-on-polymer stamping, multilayer films patterned with micron-sized features have been created.[28] However, these structures are limited to nominally two-dimensional (2-D) films that lack self-supporting features or coated colloidal particles, both of which must be compositionally modulated on the molecular length scale.

Here, we present a fundamental study of the phase behavior and rheological properties of concentrated polyelectrolyte complexes comprised of poly(acrylic acid) and poly(ethylenimine). A three-component phase diagram was constructed to reveal the region of soluble complex formation required for ink formulation. Shear viscometry and oscillatory measurements were carried out to determine the initial ink viscosity as a function of varying anionic to cationic charge ratio and the subsequent rise in ink elasticity observed upon coagulation in deposition reservoirs of varying composition. The optimal ink and reservoir chemistries were then utilized in the direct-write assembly of three-dimensional structures with micron-sized features. Our approach opens up new avenues for direct writing of complex 3-D polyelectrolyte scaffolds for a broad array of applications.

Experimental Section

Materials System. Poly(acrylic acid) (PAA) sodium salt is an anionic polyelectrolyte with a linear backbone comprised of one ionizable (COONa) group per monomer unit. PAA ($M_w \sim 10\,000$) was supplied (Polysciences, Inc., Warrington, PA) as a concentrated aqueous solution (40 wt %) and used as received for ink formulation. Poly(ethylenimine) (PEI) is a highly branched, cationic polyelectrolyte with a 1:2:1 ratio of primary, secondary, and tertiary amines, (NH_x). PEI ($M_w \sim 600$) was supplied (Polysciences, Inc.) as a concentrated liquid (99%), which was diluted with deionized water to form a concentrated aqueous solution (40 wt %) for ink formulation. The deposition reservoirs were prepared by mixing 2-propanol (IPA) (A.C.S grade, Fisher Scientific, Fair Lawn, NJ) with deionized water in varying volumetric ratios.

Phase Behavior. Concentrated polyelectrolyte complexes of varying [COONa]/[NH_x] ratio (10:1 to 1:15) were produced by mixing appropriate amounts of PAA and PEI solutions (10−40 wt %). All solutions were used at their native pH values; that is, pH was not controlled during these experiments. The number of ionizable groups per polyelectrolyte chain was calculated and converted into molar concentrations for each solution, where [COONa] = 4.2 M for PAA (40 wt %) and [NH_x] = 9.3 M for PEI (40 wt %). Immediately after mixing the PAA and PEI solutions, an opaque precipitate formed. The mixtures were equilibrated for several hours by magnetic stirring, yielding either a clear, soluble complex (single-phase), a colloidal suspension of complex particles (two-phase), or a polymer-rich precipitate with a dilute polymer-poor supernatant (two-phase).

Turbidity Measurements. Turbidity measurements were carried out on dilute PAA solutions (2 mg/mL) prepared by adding an appropriate amount of deionized water to a concentrated PAA solution (40 wt %) followed by magnetic stirring for 1 h. The desired amount of IPA was then added to this solution followed by magnetic stirring for 1 h prior to carrying out the light scattering measurements (Horiba CAPA-700, Irvine, CA). The raw data were normalized by the maximum and minimum transmitted intensity to determine the % transmittance.

Ink Rheology. The rheological properties of pure PAA solutions and PAA−PEI complexes were determined using a controlled stress rheometer (Bohlin Instruments CS-50, East Brunswick, NJ) fitted with a concentric cylinder (C14, bob diameter of 14 mm and gap width of 0.7 mm) or cone and plate (CP 4/40, cone diameter of 40 mm with a 4° angle and gap width of 0.15 mm) geometry. Their viscosity was measured in controlled stress mode using the concentric cylinder geometry. These data were acquired as a function of shear stress (τ) in a logarithmically ascending series of discrete steps (0.05−50 Pa) with a 20 s equilibrium time at each stress. All homogeneous polyelectrolyte complexes exhibited Newtonian flow behavior.

The elastic shear modulus (G') of concentrated PAA solutions and PAA−PEI complexes coagulated in deposition reservoirs of varying composition was measured by an oscillatory technique using a cone and plate geometry (CP 4/40, cone diameter of 40 mm with a 4° angle and gap width of 0.15 mm). Because these measurements could not be carried out on deposited ink filaments (1 μm diameter), we estimated that a characteristic coagulation time of ~2 h was necessary to allow a 100 μm thick film of this polyelectrolyte complex to undergo a comparable solidification reaction. These films were formed by coating the plate with the polyelectrolyte complex of interest and then dipping the cone into this viscous fluid such that both surfaces were coated with ~100 μm thick film. The coated cone and plate tools were placed in a alcohol/water coagulation reservoir (1 L) of varying composition for 2 h. They were then removed from this reservoir and mounted on the rheometer; their coated surfaces were brought into contact and fused together (5 min) prior to initiating the rheological measurement. The elastic modulus was determined by performing a stress sweep at a frequency of 1 Hz. G' values were nearly constant over a strain range of 10^{-4}−10^{-2}, and the reported values are averages taken over that range. All measurements were carried out at 22 °C using a solvent trap of appropriate composition to minimize drying effects.

Chemical Analysis. Carbon−hydrogen−nitrogen (CHN) analysis was carried out on a representative polyelectrolyte ink ([COONa]/[NH_x] = 5.7:1) before and after coagulation in different reservoirs (deionized water and 85% IPA). Coagulated samples were prepared by reacting a thin film of ink in a given reservoir for 2 h, analogous to the procedure used for the rheological measurements. Solid samples were then prepared by drying the ink in an oven at 100 °C for 12 h to fully evaporate the water and IPA. The ink composition was measured using a CHN analyzer (CE440, Exeter Analytical, Inc., North Chelmsford, MA) and compared to known values for PAA and PEI to determine the [COONa]/[NH_x] ratio.

Direct-Write Assembly. Three-dimensional (3-D) polyelectrolyte scaffolds with micron-sized features were assembled using a robotic deposition apparatus (Nanocube x−y−z micropositioner, Polytec PI, Auburn, MA). Complex 3-D patterns were defined using a computer-aided, direct-write program (IlliniCAD 3.1) that controls the three-axis micropositioner stage. The ink delivery system was mounted onto the moving x−y−z micropositioner for agile 3-D printing onto a stationary substrate. The ink is housed in a syringe (barrel diameter of 4.6 mm, EFD Inc., East Providence, RI) and robotically deposited through a pulled borosilicate glass nozzle (0.5−5 μm in diameter, μ-Tip, World

(21) Zintchenko, A.; Rother, G.; Dautzenberg, H. *Langmuir* **2003**, *19*, 2507−2513.
(22) Decher, G. *Science* **1997**, *277*, 1232−1237.
(23) Caruso, F.; Caruso, R. A.; Mohwald, H. *Science* **1998**, *282*, 1111−1114.
(24) Pei, R.; Cui, X.; Yang, X.; Wang, E. *Biomacromolecules* **2001**, *2*, 463−468.
(25) Ho, P. K. H.; Kim, J.-S.; Burroughes, J. H.; Becker, H.; Li, S. F. Y.; Brown, T. M.; Cacialli, F.; Friend, R. H. *Nature* **2000**, *404*, 481−484.
(26) Vossmeyer, T.; Guse, B.; Besnard, I.; Bauer, R. E.; Müllen, K.; Yasuda, A. *Adv. Mater.* **2002**, *14*, 238−242.
(27) Chung, A. J.; Rubner, M. F. *Langmuir* **2002**, *18*, 1176−1183.
(28) Jiang, X.; Zheng, H.; Gourdin, S.; Hammond, P. T. *Langmuir* **2002**, *18*, 2607−2615.

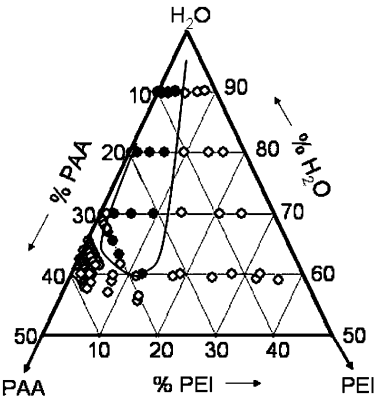

Figure 1. PAA−PEI−H_2O phase diagram showing (○) single-phase regions of macroscopically homogeneous, soluble complexes and (●) two-phase regions comprised of a turbid suspension of stable complex colloidal particles in a polymer-poor fluid (below c^*) or a precipitated complex with a polymer-poor supernatant fluid (above c^*). (Note: the solution pH ranged from pH ∼ 3.5−4 in the PAA-rich region to pH ∼ 11 in the PEI-rich region.)

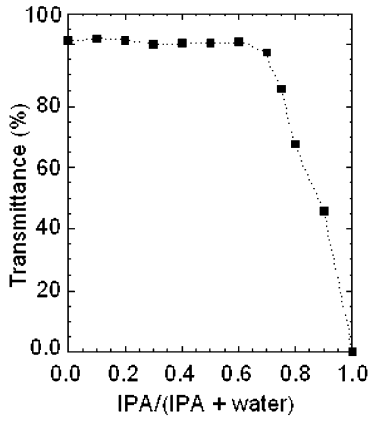

Figure 2. Turbidity of dilute PAA solutions (2 mg/mL) as a function of solvent composition, normalized to the maximum (100% water) and minimum (100% IPA) transmittance.

Precision Instruments, Inc., Sarasota, FL) under an applied pressure (800 Ultra dispensing system, EFD Inc.) to maintain a constant flow rate at a deposition speed of 20 μm/s. Higher deposition speeds were not explored due to the limited travel distance of the robotic stage (D_{max} = 100 μm for $x-y-z$). The applied pressure (15−200 kPa) varied according to the nozzle diameter and ink viscosity to achieve the desired constant deposition speed of 20 μm/s. The PAA−PEI inks were deposited in a coagulation reservoir (∼200 μL) consisting of an IPA/(IPA + water) ratio of 0.83−0.88, which is close to the azeotropic value of 0.89. As the ink exits the nozzle, it forms a continuous, rodlike filament that retains its shape after rapid coagulation (∼1 ms) in the deposition reservoir. A reservoir composition of 83−88% IPA was deemed optimal because it yielded a coagulated ink that was elastic enough to maintain its shape while spanning unsupported regions of the structure yet flexible enough to maintain flow through the deposition nozzle and adhere to the substrate and underlying layers. After patterning a given 2-D layer, the nozzle is incrementally raised in the z-direction to generate the next layer. This process is repeated until the desired 3-D structure is created.

3-D microscale periodic lattices were assembled by patterning an array of parallel (rodlike) filaments in the $x-y$ plane such that their orientation was orthogonal to the previous layer. The build time (t) varied with the size of the structure and the road width (e.g., t ∼ 1 min for four-layer structure ($x = y$ = 40 μm) with 4 μm road width and t ∼ 10 min for eight-layer structure ($x = y$ = 90 μm) with 5 μm road width). For the simple tetragonal lattices, the rod spacing (L) was varied depending on the rod size and spacing (or lattice constant) desired (L = 2−15 μm for nozzle sizes of 0.5−5 μm). All structures were dried at ∼22 °C and <35% relative humidity.

Focused ion beam milling (Strata DB 235 FIB, FEI Company, Hillsboro, OR) was used to obtain cross-sectional images of the 3-D polyelectrolyte scaffolds. First, the scaffold was located through electron beam imaging, and then, the ion beam (3000 pA current) was used to remove a defined portion of the scaffold, followed by ion milling at 500 pA to remove any excess debris, yielding a clean cross section.

Scanning electron microscopy (SEM) images were obtained with a Hitachi S-4700 scanning electron microscope (Hitachi Ltd., Tokyo, Japan). After fabrication and drying, structures were mounted and sputtered with gold for 1 min (Emitech K575 sputter coater, Emitech Ltd., Ashford Kent, U.K.) prior to imaging.

Results

Phase Behavior of PAA−PEI Complexes. The PAA−PEI−H_2O phase diagram is shown in Figure 1. Pure PAA and PEI solutions reside along binary polyelectrolyte−water tie lines. These solutions were homogeneous fluids over the entire compositional space explored. Upon mixing the PAA and PEI solutions together, dramatic differences in their phase behavior were observed. Below the dilute-to-semidilute (c^*) transition for pure PAA solutions (c^* ∼ 20 wt %), PAA−PEI complexes phase separated to yield a suspension of stable colloidal particles in water when the PEI concentration was less than or equivalent to the PAA concentration in solution. Soluble complexes formed at higher PEI concentrations, despite the lower molecular weight of PEI relative to PAA. PAA−PEI complexes that resided in the two-phase region at PAA concentrations above c^* were observed to phase separate into a polymer-rich precipitate with a polymer-poor supernatant fluid. Finally, soluble complexes formed in the PAA-rich region (∼40 wt % PAA) over a broad range of PEI additions. It should be noted that the time required to homogenize the concentrated soluble PAA−PEI complexes increased as their [COONa]/[NH_x] ratio approached the two-phase region (e.g., t_{mix} ∼ 4 h was for fluid inks prepared with a [COONa]/[NH_x] ratio of 5.7:1, whereas t_{mix} ∼ 12 h was for fluid inks prepared with a [COONa]/[NH_x] ratio of 2:1). The concentrated, PAA-rich region was identified as the most suitable for ink formulation. As stated previously, no attempt was made to control the solution pH, which ranged from pH ∼ 3.5−4 in the PAA-rich region to pH ∼ 11 in the PEI-rich region.

The phase behavior of dilute PAA solutions (∼0.01c^*) of varying composition was studied by light scattering, as shown in Figure 2. These solutions are transparent in deionized water and alcohol/water solutions (≤70 vol % IPA). At higher alcohol concentrations (>70 vol % IPA), the solutions became increasingly turbid, reflecting a dramatic change in their stability. Ultimately, the system became completely opaque in pure alcohol.

Initial Ink Rheology. The viscosity of concentrated PAA−PEI inks (total polyelectrolyte concentration of ∼40 wt % in solution) as a function of varying [COONa]/[NH_x] ratio is shown in Figure 3. Under these conditions, a narrow two-phase region consisting of a polymer-rich aggregated network and a polymer-poor fluid was observed ranging from [COONa]/[NH_x] ratios of ∼2.1 to 3.9. The rheological properties of two-phase mixtures were not investigated. All inks characterized consisted of soluble PAA−PEI complexes that exhibited Newtonian flow behavior over the experimental conditions of interest. The ink viscosity increased from roughly 1 Pa·s for a pure PAA (40 wt %) solution to 10 Pa·s for PAA−PEI complexes (∼40 wt %) with a [COONa]/[NH_x] ratio of 5. On the opposite side of the two-phase region, PAA−PEI complexes

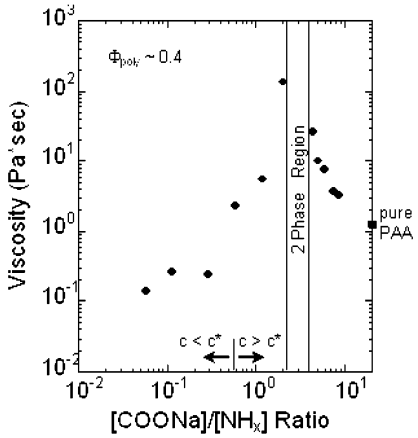

Figure 3. Log−log plot of the initial ink viscosity for concentrated polyelectrolyte complexes (40 wt %) with varying [COONa]/[NH$_x$] ratio. As a benchmark, the viscosity of a concentrated PAA solution (40 wt %) is shown (■) on the right axis.

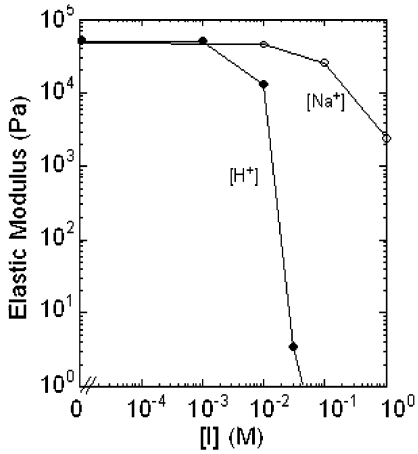

Figure 4. Log−log plot of the elastic modulus of concentrated inks (40 wt % with a 5.7:1 [COONa]/[NH$_x$] ratio, pH ~ 3.8) coagulated in aqueous reservoirs of varying ionic strength (○) or pH (●).

with a [COONa]/[NH$_x$] ratio of 2 exhibited an ink viscosity of 135 Pa·s, which was the maximum value observed. Upon further PEI addition, the ink viscosity decreased markedly as the PAA concentration was reduced below its c^* value.

Coagulated Ink Rheology. Soluble PAA−PEI complexes used as inks for direct-write assembly coagulate when deposited into a reservoir comprised of two miscible liquids, isopropyl alcohol (IPA) and deionized water, mixed together at different volumetric ratios. The observed rise in ink elasticity depended strongly on reservoir composition, as shown in Figures 4 and 5, for a representative PAA−PEI complex with a [COONa]/[NH$_x$] ratio of 5.7. Prior to coagulation, this ink exhibits a shear elastic modulus (G') of ~1 Pa. In aqueous reservoirs, the coagulated ink elasticity depends on both pH and ionic strength, as shown in Figure 4. Inks coagulated in deionized water (pH ~ 6) experienced a nearly 5-orders-of-magnitude increase in elasticity ($G' \sim 5 \times 10^4$ Pa) relative to its initial state. The observed rise in ink elasticity decreased significantly with decreasing pH, until the PAA−PEI complex dissolved completely in the reservoir under highly acidic conditions (pH < 2). The coagulated ink elasticity also depended on the salt (NaCl) concentration in the aqueous reservoir, such that the observed rise in ink elasticity decreased with increasing ionic strength. For example, the coagulated ink had a G' value of ~10^3 Pa in an aqueous reservoir with 1 M NaCl, nearly 2 orders of magnitude lower than that in a pure deionized water reservoir for a comparable coagulation time of 120 min (see Figure 4). Upon adding IPA to the pure deionized reservoir, a more complicated dependence of ink elasticity on reservoir composition was observed (see Figure 5). For water-rich reservoirs, there was a significant decrease in ink elasticity with increasing IPA content. A minimum G' value of ~10^2 Pa was observed for an alcohol/water reservoir comprised of 70% IPA. Upon further IPA addition, the ink elasticity exhibited a marked rise, with a G' value of ~10^5 Pa observed for inks coagulated in a pure IPA reservoir.

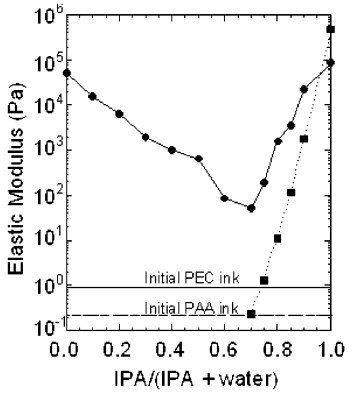

Figure 5. Semilog plot of the elastic modulus of concentrated inks (40 wt % with a 5.7:1 [COONa]/[NH$_x$] ratio) coagulated in reservoirs of varying water/IPA ratio for polyelectrolyte complex ink (●) and a concentrated PAA solution (40 wt %, ■).

Direct-Write Assembly of 3-D Polyelectrolyte Scaffolds. Concentrated polyelectrolyte complexes (~40 wt % with a [COONa]/[NH$_x$] ratio of 2−5.7) were utilized as inks for the direct-write assembly of the 3-D microperiodic structures shown in Figures 6−8. Representative images of a 3-D polyelectrolyte scaffold comprised of a simple tetragonal lattice are shown in Figure 6. The 3-D scaffold consists of spanning filaments patterned in a serpentine sequence to yield parallel rods oriented orthogonally between layers and porous outer walls. These scaffolds, patterned within the deposition reservoir, maintain their structural integrity during the drying process. Through focused ion beam milling, we can subsequently sculpt these scaffolds into various forms by removing defined sections, for example, a triangular slice (Figure 6c). This sculpting procedure yielded the cross-sectional view shown in Figure 6d, which reveals the filament−filament interfaces formed between patterned layers. By varying the deposition parameters (see Table 1), 3-D scaffolds can be built with varying feature size. Three-dimensional periodic scaffolds with minimum and maximum filament diameters between ~0.6 and 6.0 μm have been constructed, as shown in Figure 7. The characteristic filament size is slightly larger than the nozzle diameters ($D = 0.5-5.0$ μm) used to direct-write such structures, in each case. By altering the reservoir composition, 3-D scaffolds with a highly porous architecture can also be created, as shown in Figure 8.

Discussion

Concentrated polyelectrolyte inks were developed for the direct-write assembly of 3-D microperiodic scaffolds that flow through fine deposition nozzles and then rapidly coagulate in a deposition reservoir to create self-supporting filaments (or rods). We first discuss compositional effects on the phase behavior and rheological properties of

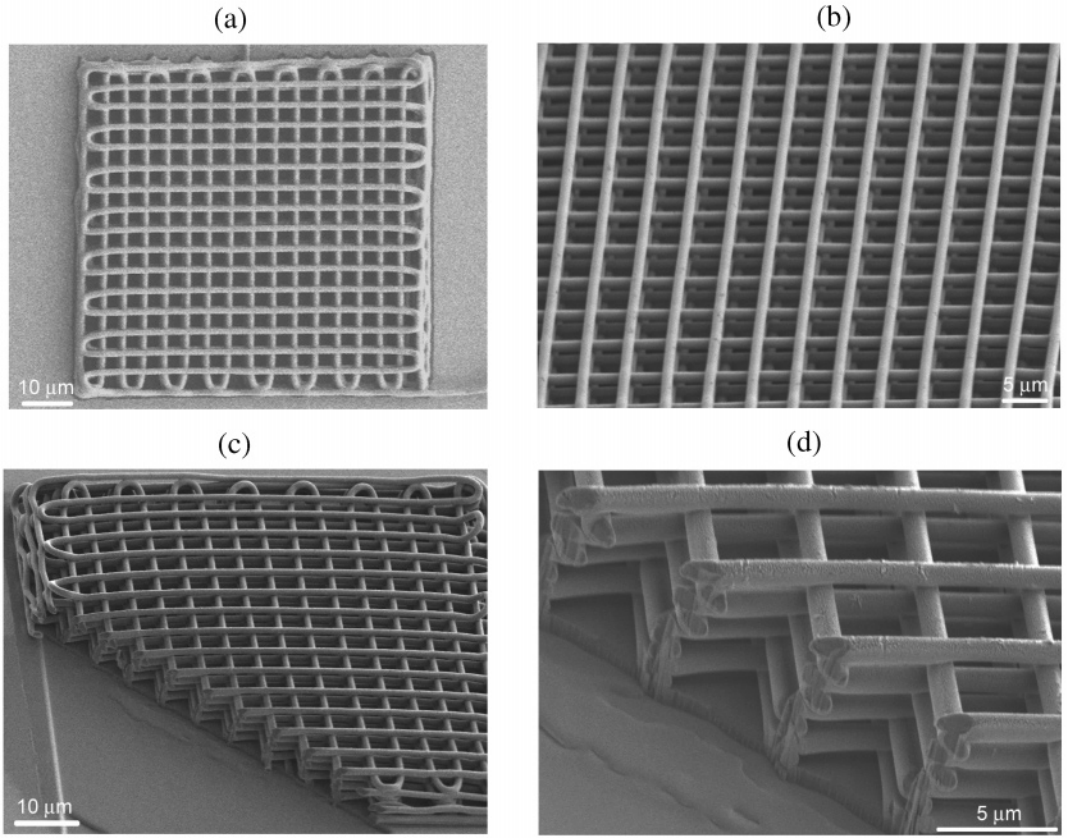

Figure 6. SEM images of 3-D periodic structures with simple tetragonal symmetry (filament diameter, 1 μm; road width, 5 μm; eight layers): (a) top view revealing registration between layers; (b) angled view showing several layers of spanning filaments; (c) triangular section removed with focused ion beam milling; (d) close-up of a cut exposing the high integrity interfaces formed between layers.

polyelectrolyte complexes, followed by a discussion of ink flow during deposition and reservoir effects on ink coagulation. Finally, we highlight areas of future opportunity for direct writing 3-D polyelectrolyte scaffolds.

Composition Effects on PAA−PEI Complexes. To create concentrated soluble complexes suitable for 3-D writing, PAA and PEI solutions were mixed together under conditions that promoted polyelectrolyte exchange reactions; that is, the polyions possessed significant differences in their molecular weights, there was an excess of the higher molecular weight species (PAA), and the solution pH and ionic strength facilitated structural rearrangements between polyions in solution. In these complexes, PAA served as the lyophilizing (host) polyelectrolyte and PEI served as the blocking (guest) polyelectrolyte.[16,29] All PAA−PEI complexes were turbid (or aggregated) upon initial mixing. The evolution of a soluble complex from this highly aggregated, initial state was recently studied by Zintchenko et al.[21] They found that the dissolution kinetics depended strongly on the polyelectrolyte concentration, salt concentration, and mixing ratio. The following model was proposed to explain their findings. After initial mixing, the complex consists of aggregated particles (or a network at higher concentrations) with a nearly 1:1 charge ratio and an excess of "free" lyophilizing species in solution. The system then undergoes structural rearrangements as it evolves toward a uniform distribution of the lower M_w component among chains of the higher M_w component. Soluble complexes emerge only when polyelectrolyte exchange reactions are favored and there is a sufficient excess of the lyophilizing species. For the concentrated PAA−PEI complexes (40 wt %) studied, their dissolution time increased from ~1 to 12 h as the [COONa]/[NH_x] ratio decreased from ~5.7 to 2. The initial aggregated network persisted over long times (≫days) at intermediate [COONa]/[NH_x] ratios of ~2.5−4.5. Phase separation likely occurred at higher PAA concentrations (>1:1 ratio), because the polyanions are not fully charged under these pH conditions.

Interestingly, PAA−PEI complexes formed at lower PAA concentrations (<c^*) required only minor PEI additions to induce phase separation into a suspension of colloidal particles. In great contrast, soluble complexes formed at higher PAA concentrations (≥c^*) could accommodate much larger additions of the blocking (guest) polyelectrolyte, PEI, without phase separating. This is clearly shown in the PAA−PEI−H_2O phase diagram (see Figure 1), where the phase boundary between soluble complex formation and the two-phase region shifts from ~1 to 10 wt % PEI as the PAA concentration increases from 30 to 40 wt % in solution. This trend is attributed to enhanced exchange reactions that occur due to increased counterions (e.g., Na^+) at higher PAA concentrations. Concentrated PAA−PEI complexes rich in the lyophilizing species, PAA, therefore yielded a broader compositional range for ink formulation.

Ink Flow during Deposition. By regulating the [COONa]/[NH_x] ratio within the PAA−PEI complex, their initial viscosity could be tailored over the wide range needed to facilitate ink flow through microscale deposition nozzles of varying diameter (see Table 1). If there were no interactions between oppositely charged species, one would expect the viscosity to be dominated by the PAA concentration in solution. In this case, the ink viscosity

(29) Bakeev, I. H.; Izumrudov, V. A.; Kuchanov, S. I.; Zezin, A. B.; Kabanov, V. A. *Macromolecules* **1992**, *25*, 4249−4254.

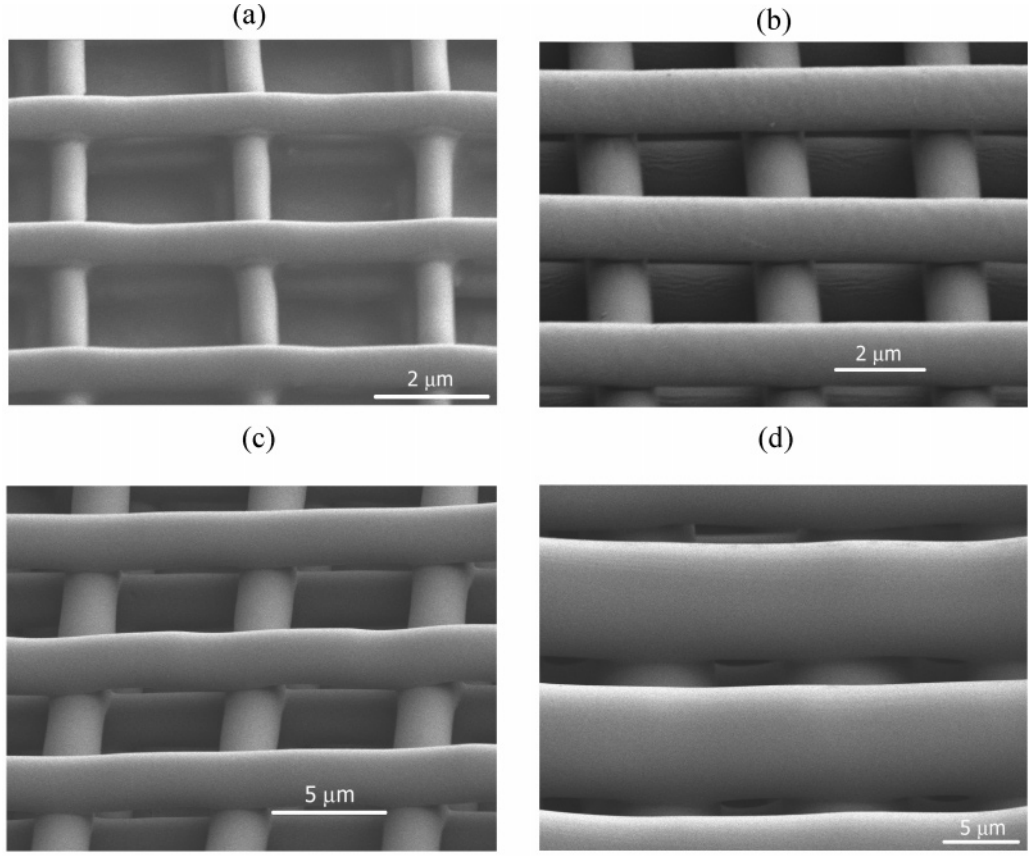

Figure 7. SEM images of 3-D simple tetragonal structures assembled with varying filament diameters by varying the [COONa]/[NH_x] ratio of the inks: (a) 0.6 μm filaments, [COONa/NH_x] = 5.7:1; (b) 1.2 μm filaments, [COONa/NH_x] = 5.7:1; (c) 2.4 μm filaments, [COONa/NH_x] = 5:1; (d) 6.6 μm filaments [COONa/NH_x] = 2:1.

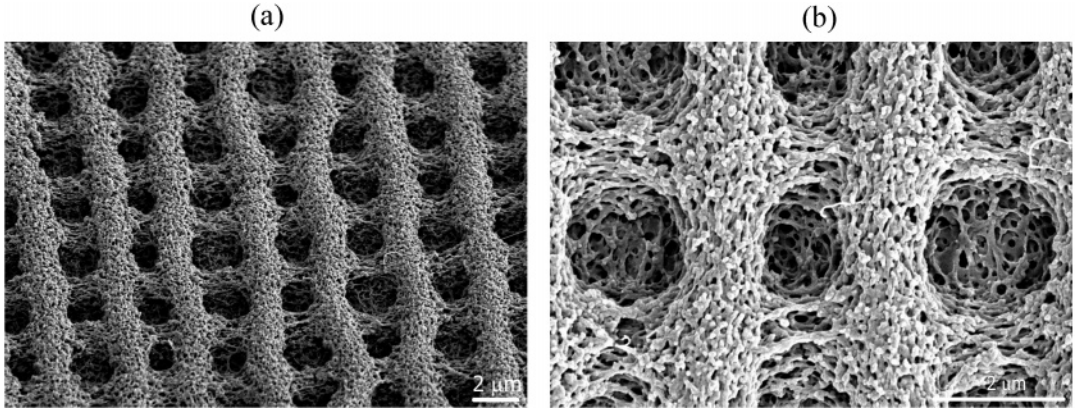

Figure 8. SEM images of highly porous periodic structures assembled in a slightly acidic (pH < 3) aqueous reservoir.

Table 1. Deposition Parameters for Polyelectrolyte Inks

polyelectrolyte ink [COONa/NH_x]	ink viscosity (Pa·s)	nozzle diameter (μm)	applied pressure (kPa)	estimated pressure (kPa)
5.7:1	7.6	0.5	170	105
5.7:1	7.6	1.0	70	50
5:1	10.1	2.0	15	9
2:1	135.0	5.0	15	19

should not exceed the measured value of ~1 Pa·s obtained for the concentrated PAA solution (40 wt %); that is, the ink viscosity should decrease rapidly with decreasing PAA content as the overlap between polyanion chains lessens above c^*, whereas a linear dependence of ink viscosity on PAA concentration is expected below c^*. In sharp contrast, a significant rise in ink viscosity was observed on either side of the two-phase region (see Figure 3) with all PAA-rich complexes ($>c^*$) exhibiting higher Newtonian viscosities than pure PAA solutions at the same polyion concentration (40 wt %). These observations are in qualitative agreement with the rheological behavior reported by Winnik and co-workers[30] for other semidilute polymer complexes. They suggest that the observed rise in viscosity near the two-phase boundary stems from the interactions between polyion chains, which fosters some type of molecular-level structuring in solution.[30] Its exact nature would likely depend on several factors including the polyion concentration, architecture, mixing ratio, and solution conditions.

The laminar flow of viscous inks through a cylindrical tube can be described by the Hagen−Poiseuille equation:[31]

(30) Liu, R. C. W.; Morishima, Y.; Winnik, F. M. *Macromolecules* **2001**, *34*, 9117−9124.

$$Q = \pi R^4 \Delta p / 8 \eta L \quad (1)$$

where Q is the volumetric flow rate, R is the tube radius, Δp is the pressure drop, η is the ink viscosity, and L is the length of the tube. Our deposition nozzles consist of long tapered capillaries whose radii gradually decrease to the final nozzle size. Because the capillary radius far exceeds the nozzle radius, the pressure drop can be estimated using the following relationship for flow through a slowly varying channel:[31]

$$\Delta p = \frac{8\eta Q}{\pi} \int_{x_1}^{a} R^{-4}\, dx \quad (2)$$

where a is the nozzle radius and x_1 is the capillary radius. In this case, R varies with x according to

$$R = x \tan(\alpha) \quad (3)$$

where α is the angle of taper. Solving the integral yields

$$\Delta p = \frac{8\eta Q}{3\pi(\tan \alpha) a^3} \quad (4)$$

where the pressure drop at x_1 can also be neglected because x_1 is much greater than a. This relation assumes a sufficiently small α value and also neglects inertial forces, which is valid for the ink and deposition parameters used in this study, since

$$\alpha \frac{2\rho Q}{\pi a \eta} \ll 1 \quad (5)$$

Using the above expressions, we estimated the pressure required to maintain the desired volumetric flow rate ($Q = \nu \pi R^2$) at a constant deposition speed (ν) of 20 μm/s (see Table 1). For comparison, the actual applied pressures utilized for each set of deposition conditions studied are also reported. As expected, the pressure required to maintain a given flow rate increased with increasing ink viscosity or decreasing nozzle diameter. To date, 3-D structures have been fabricated through deposition nozzles ranging from 0.5 to 5 μm in diameter (Figure 7). Upon further manipulation of important variables, such as the polyelectrolyte composition, molecular weight, and concentration, it should be possible to create structures with feature sizes ranging from 100 nm (desired ink viscosity of ~0.4 Pa·s) to 10 μm (desired ink viscosity of ~400 Pa·s). These targeted viscosity values were estimated assuming respective deposition pressures of 250 and 15 kPa.

Reservoir Effects on Ink Coagulation. The ink coagulation mechanism is governed by many competing factors that depend strongly on reservoir composition. In deionized water reservoirs (pH ~ 6, low ionic strength), ink coagulation is driven by intensified electrostatic interactions between oppositely charged polyions. This mechanism results in the formation of a near-stoichiometric polyelectrolyte complex, as excess PAA, Na^+ ions, and minor amounts of PEI diffuse into the reservoir. Chemical (CHN) analysis indicated that the [COONa]/[NH_x] ratio of the coagulated ink was ~2.5, which was significantly less than its initial ratio of ~6 prior to deposition. By adding NaCl to the aqueous reservoir, ink coagulation was moderately reduced as the electrostatic attractions between polyions were better screened. Alternately, ink coagulation could also be dramatically suppressed by lowering the reservoir pH. The pK_a of PAA is ~6;[32,33] however, it has been shown both experimentally[34−39] and theoretically[40,41] that the pK_a of weak polyions is highly dependent on its local environment (e.g., near charged surfaces[34,35] or within multilayers[36−39]). For example, Burke and Barrett[39] recently reported that PAA could change its pK_a value by multiple pH units in the presence of oppositely charged polyelectrolytes (e.g., poly(allylamine) hydrochloride (PAH)) in multilayer films. Under highly acidic conditions, the carboxylic acid groups along the PAA backbone become protonated, thus breaking bonds with amine groups on the PEI chains.[39] At pH 3, there was little difference in the ink elasticity compared to that observed for inks coagulated in deionized water. Although the internal pK_a for PAA in our system was not measured, this result, combined with the elemental analysis, suggests that not all carboxylic acid groups need to participate in complexation to induce a large rise in ink elasticity. At pH 2, the rise in ink elasticity was considerably reduced as the PAA backbone was further protonated, and over time, the ink began to slowly dissolve in the reservoir. At pH 1, where PAA species are negligibly ionized, the ink quickly dissolved in the reservoir. This phenomenon was exploited to create the highly porous 3-D scaffolds shown in Figure 8. Other groups have observed similar behavior in polyelectrolyte multilayers.[42,43] For example, Mendelsohn et al.[42] found that brief immersion of PAA/PAH multilayers in an acidic reservoir caused the films to rearrange to form thick, highly porous membranes.

The ink elasticity also depends strongly on the dielectric properties of the reservoir, as observed in alcohol/water mixtures. In reservoirs ranging from pure water and 70% IPA, there was a systematic reduction in ink elasticity with increasing IPA content. Again, similarities can be drawn from work on polyelectrolyte multilayers. Poptoshev et al.[44] found that multilayers of PAH and poly(styrenesulfonate sodium salt) (PSS) grew more rapidly as the ethanol content of their adsorption baths increased. They attributed this to a progressive screening of the intrachain electrostatic interactions due to the decreased dielectric constant of the medium, resulting in thicker adsorbed layers. We believe that enhanced counterion condensation might play a role in suppressing the rise in ink elasticity observed for alcohol/water reservoirs (0−70% IPA).[45] If Na^+ counterions remain associated with the PAA backbone, the electrostatic interactions between oppositely charged PAA and PEI species in the ink would be weakened. Unambiguously determining the role of electrostatic interactions in mixed solvent reservoirs is beyond the scope of this work, but this clearly has

(31) Batchelor, G. K. *An Introduction to Fluid Dynamics*; Cambridge University Press: Cambridge, U.K., 2000.
(32) Gregoy, H. P.; Frederick, M. *J. Polym. Sci.* **1957**, *23*, 451−465.
(33) Kirby, G. H.; Harris, D. J.; Li, Q.; Lewis, J. A. *J. Am. Ceram. Soc.* **2004**, *87*, 181−186.
(34) Hoogeveen, J. G.; Cohen Stuart, M. A.; Fleer, G. J. *J. Colloid Interface Sci.* **1996**, *182*, 133−145.
(35) Sukhishvili, S. A.; Chechik, O. S.; Yaroslavov, A. A. *J. Colloid Interface Sci.* **1996**, *178*, 42−46.
(36) Xie, A. F.; Granick, S. *Macromolecules* **2002**, *35*, 1805−1813.
(37) Kharlampieva, E.; Sukhishvili, S. A. *Langmuir* **2003**, *19*, 1235−1243.
(38) Sui, Z.; Schlenoff, J. B. *Langmuir* **2004**, *20*, 6026−6031.
(39) Burke, S. E.; Barrett, C. J. *Langmuir* **2003**, *19*, 3297−3303.
(40) Bohmer, M. R.; Evers, O. A.; Scheutjens, J. M. H. M. *Macromolecules* **1990**, *23*, 2288−2301.
(41) Cohen Stuart, M. A.; Fleer, G. J.; Lyklema, J.; Nore, W.; Scheutjens, J. M. H. M. *Adv. Colloid Interface Sci.* **1991**, *34*, 477−535.
(42) Mendelsohn, J. D.; Barrett, C. J.; Chan, V. V.; Pal, A. J.; Mayes, A. M.; Rubner, M. F. *Langmuir* **2000**, *16*, 5017−5023.
(43) Sukhishvili, S. A.; Granick, S. *J. Am. Chem. Soc.* **2000**, *122*, 9550−9551.
(44) Poptoshev, E.; Schoeler, B.; Caruso, F. *Langmuir* **2004**, *20*, 829−834.
(45) Manning, G. S. *Acc. Chem. Res.* **1979**, *12*, 443−449.

important implications for both direct-write assembly[1] and electrostatic-driven layer-by-layer assembly[22] of polyelectrolyte-based structures.

In alcohol-rich reservoirs (>70% IPA), ink coagulation is driven by solvent quality effects. Generally, in polyelectrolyte solutions, decreases in the electrostatic repulsions between the chain segments, either by increasing the ionic strength[46] or by decreasing the dielectric constant[47] of the medium, cause transitions in the polymer conformation from extended coils to globules.[48] The extent of this collapse increases as the solvent quality decreases, eventually leading to precipitation and phase separation.[44] This mechanism does not yield a nearly stoichiometric complex with excess polyelectrolyte species dissolved in the reservoir. Rather, the entire complex aggregates together with a [COONa]/[NH_x] ratio equivalent to that found in the initial ink, as determined by chemical (CHN) analysis. The solvent quality mechanism is further supported by the data shown in Figures 2 and 5, which depict turbidity measurements carried out on dilute PAA solutions of varying IPA concentration and the rise in the elastic modulus of concentrated PAA (40 wt %) solutions during coagulation in alcohol-rich reservoirs, respectively. Below 70% IPA, the dilute PAA solutions remained transparent (or stable), while the concentrated PAA solutions simply dissolved in the reservoir. As the IPA content in the reservoir was enriched above 70%, there was a simultaneous increase in both the turbidity and the elasticity of dilute and concentrated PAA solutions, respectively, indicative of coagulation. These observations reveal that PAA species will aggregate (even in the absence of oppositely charged PEI species) in IPA-rich solutions solely due to solvent quality effects.

Implications on Direct-Write Assembly. The design of concentrated polyelectrolyte inks comprised of viscous fluids that coagulate to yield highly elastic filaments upon contact with a deposition reservoir is central to our direct-write assembly technique. These inks must possess the appropriate viscosity to facilitate flow under modest applied pressures. Several parameters can be manipulated to tailor the ink viscosity, including the polyion molecular weight, concentration, and mixing ratio. However, the concentration of the lyophilizing polyelectrolyte should reside above c^* for the coagulation reaction to yield solid filaments rather than colloidal particles in suspension. Coagulation must also be rapid and produce filaments with the appropriate stiffness to maintain their shape and span unsupported regions during deposition and flexibility to adhere to the substrate or underlying layers within the scaffold. Looking toward the future, many ink and reservoir chemistries can be envisioned, including those based on physical (e.g., electrostatic and solvent quality) or chemical (e.g., polymerization) gelation. The inherent flexibility of direct-write assembly offers the potential to pursue a myriad of applications that either require or could benefit from 3-D architectures.

Conclusions

We have developed concentrated polyelectrolyte inks for the direct-write assembly route of 3-D microperiodic structures. By carefully tuning the ink and reservoir chemistries, soluble polyelectrolyte complexes were created that exhibit the desired fluidity required for flow through microscale deposition nozzles yet could be rapidly coagulated in situ during deposition to facilitate shape retention of the extruded filaments. This technique offers great promise for the future, as other polyelectrolyte mixtures, including those based on electrically, optically, or biologically active polyelectrolytes, can be imagined by rational extension. We expect that the ability to construct 3-D structures of arbitrary design and functionality will open up yet unexplored avenues for the direct-write assembly of photonic or fluidic systems, sensor arrays, and bioscaffolds.

Acknowledgment. This material is based on work supported by the U.S. Department of Energy, Division of Materials Sciences, under Award No. DEFG-02-91ER45439, through the Frederick Seitz Materials Research Laboratory at the University of Illinois at Urbana-Champaign. The authors also acknowledge use of the facilities at the Center for Microanalysis of Materials. G.M.G. was supported by an NDSEG fellowship. We thank J. Gilchrist and M. Roberts for useful discussions.

LA048228D

(46) Dobrynin, A. V.; Rubinstein, M.; Obukhov, S. *Macromolecules* **1996**, *29*, 2974−2979.

(47) Micka, U.; Holm, C.; Kremer, K. *Langmuir* **1999**, *15*, 4033−4044.

(48) Kiriy, A.; Gorodyska, G.; Minko, S.; Jaeger, W.; Stepanek, P.; Stamm, M. *J. Am. Chem. Soc.* **2002**, *124*, 13454−13462.